

Electronic Raman scattering in p -doped GaAs/Ga_{1-x}Al_xAs quantum-well structures: Scattering mechanisms and many-particle interactions

C. Schüller, J. Kraus, and G. Schaack

Physikalisches Institut der Universität Würzburg, 97074 Würzburg, Federal Republic of Germany

G. Weimann

Walter-Schottky-Institut der Technischen Universität München, 85748 Garching, Federal Republic of Germany

K. Panzlaff

Abteilung Optoelektronik der Universität Ulm, 89075 Ulm, Federal Republic of Germany

(Received 18 August 1994)

By means of resonance Raman spectroscopy we have investigated intersubband transitions of quasi-two-dimensional (2D) hole gases in p -type modulation-doped GaAs/Ga_{1-x}Al_xAs quantum-well structures. The observed excitations have an essentially single-particle character due to Landau damping of collective excitations and due to single-particle scattering by energy-density fluctuations under conditions of extreme resonance. In samples with well widths of typically 100 – 200 Å and 2D hole densities $p \sim 10^{11} \text{ cm}^{-2}$, we observe a characteristic variation of intersubband-transition energies with laser frequency in depolarized and in polarized scattering configurations. This variation is caused by the nonparabolic subband dispersion of the 2D single-particle hole subbands. Experiments under variation of p , by illuminating the sample with photons that have energies above the band gap of the Ga_{1-x}Al_xAs barriers, allow an estimate of the relative strengths of direct and exchange Coulomb interactions. From these experiments a greater relative strength of the exchange interaction, in comparison to that found for 2D electron gases, can be deduced.

INTRODUCTION

In inelastic light scattering experiments one can observe intersubband excitations of two-dimensional (2D) carrier systems in semiconductor quantum-well structures. These excitations can be of collective type, so-called spin-density (SDE's) and charge-density excitations (CDE's), or they can be single-particle excitations (SPE's). CDE's are shifted with respect to the corresponding SPE due to direct and exchange Coulomb interactions. The total amount of the corresponding collective shift depends on the relative and total strengths of direct and exchange Coulomb interactions. SDE's have shifts to lower energies due to exchange interaction.¹⁻⁷ The difference in excitation energy between SDE's and CDE's belonging to the same intersubband transition is called depolarization shift. CDE's and SDE's can be separated experimentally by polarization selection rules. Excitations of collective character only exist if energetically well separated from the spectrum of SPE's (single-particle continuum), whose width depends on the transferred in-plane wave vector and on the shape of the single-particle subband dispersion. Within a single-particle continuum the collective excitations (SDE's and CDE's) decay into uncorrelated electron-hole pairs⁸⁻¹⁵ (Landau damping).

Many-particle interactions in 2D electron gases in n -doped quantum-well structures have been extensively investigated by Raman spectroscopy (see, e.g., Refs. 7, 11-14). These experiments demonstrated the importance of both the direct and exchange Coulomb interaction for

determination of intersubband-transition energies of 2D electron gases in n -doped GaAs/Ga_{1-x}Al_xAs quantum-well systems. In contrast, only a little information is available about 2D hole gases. By means of resonance Raman spectroscopy we have investigated intersubband transitions of the 2D hole gas of p -type modulation-doped GaAs/Ga_{1-x}Al_xAs quantum-well structures. The most important feature of such systems is the strongly nonparabolic subband dispersion of the single-particle hole subbands due to mixing of heavy- and light-hole bands for $\mathbf{k}_{\parallel} \neq 0$ (\mathbf{k}_{\parallel} means the in-plane wave vector).¹⁶ This nonparabolicity is definitely not negligible in the case of p -doped samples of any material with zinc-blende or diamond structure^{9,17-20} and also has to be taken into consideration for n -doped quantum-well structures with narrow band gap.²¹ Magnetotunneling spectroscopy, and hot-electron-acceptor luminescence,²²⁻²⁴ were recently described as techniques which are able to probe the complicated dispersion curves of hole states in 2D systems, where these methods can even study the cubic anisotropy.²⁴⁻²⁶ For intersubband-transition energies of 2D hole systems measured by resonance Raman spectroscopy the subband nonparabolicity results in a characteristic variation of the observed transition energies (in depolarized as well as in polarized geometry) with laser energy as reported previously.^{17,18} We briefly discuss this consequence of subband nonparabolicity in this publication. Special attention in the present work is paid to the influence of the nonparabolic subband dispersion on the scattering mechanisms for resonant exci-

tation and hence on the character (collective or single-particle) of the observed excitations. The first investigations of intersubband excitations of 2D hole gases in GaAs/Ga_{1-x}Al_xAs quantum-well structures by Raman spectroscopy were made by Pinczuk and co-workers.^{19,27} These authors found that collective effects are of minor importance in these samples. Their experiments showed that for quite high hole densities ($p = 5.8 \times 10^{11} \text{ cm}^{-2}$) the depolarization shift is smaller than for lower densities ($p = 2 \times 10^{11} \text{ cm}^{-2}$) in contrast to theory.²⁰ Theoretical calculations of Ando²⁰ predict that the depolarization shift should increase with increasing carrier concentration p , as is the case in the 2D electron gas in n -doped samples. We assume that the decreasing depolarization shift in these experiments may be due to stronger Landau damping of collective excitations at high doping concentrations.⁹ For $p = 5.8 \times 10^{11} \text{ cm}^{-2}$ the single-particle continua of intersubband excitations are quite broad, even for in-plane wave vector transfers $\mathbf{q} = \mathbf{0}$ (vertical excitations in \mathbf{k}_{\parallel} space), so that the collective excitations partly overlap the continuum of SPE's and hence are strongly Landau damped. In samples of lower hole density ($p \leq 2 \times 10^{11} \text{ cm}^{-2}$), as investigated in this work, we assume that the single-particle character of the hole excitations also dominates, again due to Landau damping of collective excitations and due to strong single-particle scattering by energy-density fluctuations under conditions of extreme resonance. The scattering by energy-density fluctuations is caused by the nonparabolic subband dispersion of the 2D hole subbands.

For a detailed discussion of this we provide some general theoretical considerations in the following section about scattering mechanisms (Sec. IA) and especially about resonant single-particle scattering (Sec. IB) in p -doped GaAs/Ga_{1-x}Al_xAs quantum-well structures, taking into account the strong nonparabolicity of 2D single-particle hole subbands. In Sec. II our experimental results are described. The effects of subband nonparabolicity on intersubband-transition energies are briefly discussed (Sec. IIA). Furthermore, the effects of many-particle interactions on intersubband-transition energies have been investigated. An estimation of the relative strengths of direct and exchange Coulomb interaction is given (Sec. IIB). Finally the results are summarized in Sec. III.

I. THEORETICAL CONSIDERATIONS

In this section some theoretical considerations are given to explain the dominant single-particle character of the observed intersubband excitations. In Sec. IA the scattering mechanisms which may contribute to resonant inelastic light scattering by intersubband excitations in p -doped GaAs/Ga_{1-x}Al_xAs quantum-well structures are discussed. The inelastic scattering of light in 2D carrier systems is due to various density fluctuations of the carrier system.²⁸ The strong nonparabolicity of single-particle hole subbands may be responsible for relatively strong single-particle scattering by unscreened energy-density fluctuations (see below). In Sec. IB the con-

sequence of nonparabolicity for intersubband-transition energies for resonant single-particle scattering is investigated theoretically. These investigations confirm the interpretation of the experimentally detected, characteristic variation of intersubband-transition energies with laser energy reported previously^{17,18} as an effect of the nonparabolic dispersion of the single-particle hole subbands (see also Sec. II).

A. Scattering mechanisms

(a) *Spin-density and charge-density fluctuations.* In Fig. 1 the transitions, which contribute to the resonant single-particle scattering by charge-density fluctuations (CDF's) and spin-density fluctuations (SDF's) in the two-step (a) and three-step (b) carrier-density scattering mechanism,²⁸ are sketched. In the two-step mechanism a hole is excited from the $i = 0$ subband to the $i = 1$ subband (a). In the third step of the three-step mechanism (b) the excitation energy of the SPE is transferred to another SPE due to direct Coulomb interaction (Coulomb screening) or exchange interaction (exchange screening). This process represents the screening of the SPE by other SPE's.²⁸ In systems with parabolic subband dispersion the screening of SPE's is nearly complete.

In the scattering by *collective excitations* (SDE's and CDE's), the photoexcited hole couples in the third step of the three-step mechanism to the SDF's and CDF's of the system.⁶ Scattering due to SDF's is observed in depolarized scattering geometry ($\mathbf{e}_i \perp \mathbf{e}_s$) and scattering due to CDF's in the polarized scattering configuration²⁹ ($\mathbf{e}_i \parallel \mathbf{e}_s$), where \mathbf{e}_i (\mathbf{e}_s) means the polarization direction of the incident (scattered) beam.

(b) *Energy-density fluctuations.* In strongly nonparabolic systems another scattering mechanism, due to so-called energy-density fluctuations (EDF's), becomes important.^{30,31} The scattering efficiency for resonant scattering by density fluctuations is proportional to^{32,33}

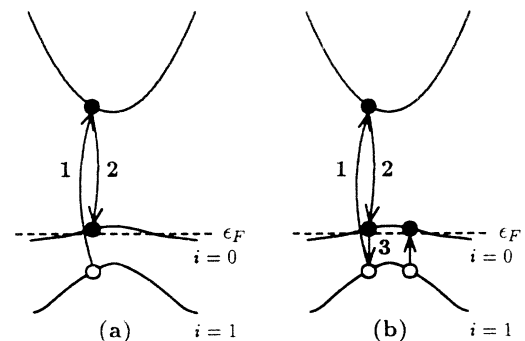


FIG. 1. Schematic representation of single-particle transitions, which contribute to the two-step (a) and three-step (b) carrier-density scattering mechanism (Ref. 28) of the resonant inelastic light scattering process in 2D hole gases. In (a) a hole is excited from the $i = 0$ subband to the $i = 1$ subband. The third step in (b) represents the screening of the single-particle transition by other single-particle transitions.

$$\frac{\partial^2 \sigma}{\partial \Omega \partial \omega} \sim \left(\frac{\omega_i}{\omega_s} \right) \int_{-\infty}^{\infty} e^{i\omega t} \langle N(t) N(0) \rangle dt, \quad (1)$$

$$N = \sum_{\alpha\beta} \gamma_{\alpha\beta} C_{\beta}^{\dagger} C_{\alpha}, \quad (2)$$

where $N(t)$ means the time-dependent operator in the Heisenberg picture corresponding to N , which is the generalized density-fluctuation operator. ω_i (ω_s) is the frequency of the incident (scattered) light and C_{β}^{\dagger} (C_{α}) are creation (annihilation) operators of the single-electron states (Bloch states). If the scattering amplitude $\gamma_{\alpha\beta}$ is independent of \mathbf{k}_{\parallel} (e.g., far away from resonance) the effective interaction Hamiltonian which is responsible for the scattering of light by the carrier system can be split into a part which corresponds to the coupling of the electromagnetic field to SDF's and a part which describes the coupling to CDF's.³³ Under conditions of *extreme resonance*, however, this means the energy of the incoming laser photons is nearly equal to the effective energy band gap between valence and conduction band, $\gamma_{\alpha\beta}$ takes the form³²

$$\gamma_{\alpha\beta} \sim \frac{1}{m} \sum_{\beta'} \left(\frac{\langle \alpha | \mathbf{e}_i \cdot \mathbf{p} | \beta' \rangle \langle \beta' | \mathbf{p} \cdot \mathbf{e}_s | \beta \rangle}{\varepsilon_{\alpha} - \varepsilon_{\beta'} - \hbar\omega_i} + \frac{\langle \alpha | \mathbf{e}_s \cdot \mathbf{p} | \beta' \rangle \langle \beta' | \mathbf{p} \cdot \mathbf{e}_i | \beta \rangle}{\varepsilon_{\alpha} - \varepsilon_{\beta'} + \hbar\omega_i} \right), \quad (3)$$

where the sum, in principle, runs over all intermediate states β' with energy $\varepsilon_{\beta'}$. m means the free electron mass. Due to the resonance denominator in Eq. (3), contributions from transitions $\alpha \rightarrow \beta$, with $\varepsilon_{\alpha} - \varepsilon_{\beta'} \approx \hbar\omega_i$, dominate the scattering amplitude $\gamma_{\alpha\beta}$. In the case discussed in this paper, the resonant intermediate state $|\beta'\rangle$ belongs to the c_1 conduction band subband. $\gamma_{\alpha\beta} = \gamma_{\alpha\beta}(\mathbf{k}_{\parallel})$ since the dispersion relations $\varepsilon(\mathbf{k}_{\parallel})$ [see Fig. 2(a)] as well as the wave functions, which determine the matrix elements in Fig. 2(b), of the 2D hole system depend on \mathbf{k}_{\parallel} . This is responsible for a scattering mechanism which causes scattering by unscreened SPE's and which is called scattering due to energy-density fluctuations.

The curves displayed in Fig. 2(a) for the subband dispersion and in Fig. 2(b) for the square of momentum matrix elements between valence- and conduction-band states are calculated within $\mathbf{k} \cdot \mathbf{p}$ formalism for a single quantum well with GaAs well width $L_z = 106$ Å and 2D hole density $p = 2.1 \times 10^{11}$ cm⁻². The Al content x of the Ga_{1-x}Al_xAs barriers was chosen as $x = 0.32$. Heavy-hole states are labeled as h_i corresponding to their character at $\mathbf{k}_{\parallel} = 0$, where i gives the subband quantum number. Correspondingly light-hole states are labeled l_i .

Thus the nonparabolicity of the 2D hole subbands in GaAs/Ga_{1-x}Al_xAs quantum-well structures has mainly two important effects concerning resonant inelastic light scattering by density fluctuations.

(i) Due to resonant scattering by energy-density fluctuations SPE's may contribute considerably to the light scattering spectra of intersubband excitations in addition to collective SDE's and CDE's, which occur due to scattering by spin-density and charge-density fluctuations.

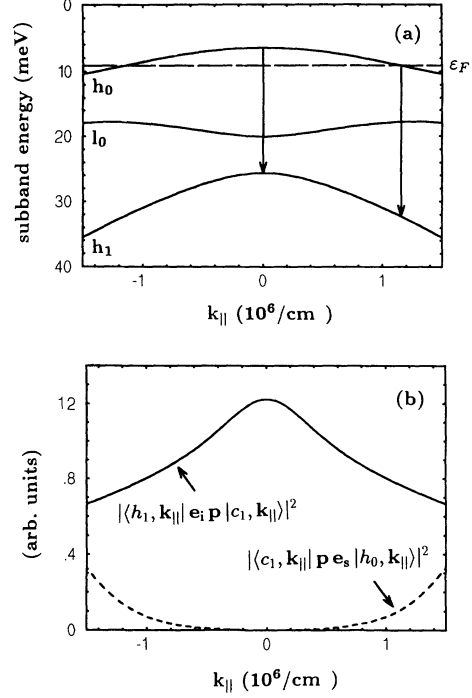


FIG. 2. Dispersion of the h_0 , l_0 , and h_1 subband of a single quantum-well structure with $L_z = 106$ Å and $p = 2.1 \times 10^{11}$ cm⁻² calculated for the flat band case (a). The arrows mark single-particle transitions with minimal (at $\mathbf{k}_{\parallel} = 0$) and maximal possible energy (at $\mathbf{k}_{\parallel} = \mathbf{k}_F$). In (b) the dependence of momentum matrix elements of single-particle transitions, which contribute to the scattering by ($h_0 \rightarrow h_1$) single-particle excitations [see also Fig. 1(a)], from the in-plane wave vector \mathbf{k}_{\parallel} is shown.

(ii) SDE's and CDE's are Landau damped because they, at least partly, lie within the continuum of SPE's (see also Fig. 7 below). For the nonparabolic single-particle hole subbands, the continuum of SPE's has even for vertical transitions, i.e., $\mathbf{q} = 0$, a finite width and so the collective SDE's and CDE's overlap the single-particle continuum and are hence Landau damped, even for $\mathbf{q} = 0$.

B. Resonant single-particle scattering

The scattering efficiency for scattering by noninteracting particles can be written in the form³²

$$\frac{\partial^2 \sigma}{\partial \Omega \partial \omega} \sim \sum_{\mathbf{k}_{\parallel}} |\gamma_{\alpha\beta}|^2 \text{Im} \left[\frac{f_{\beta} - f_{\alpha}}{\hbar\omega + \varepsilon_{\beta} - \varepsilon_{\alpha}} \right], \quad (4)$$

where in the scattering process at a wave vector \mathbf{k}_{\parallel} , with $|\mathbf{k}_{\parallel}| < |\mathbf{k}_F|$ (Fermi wave vector), a single particle is excited from a state with subband energy $\varepsilon_{\alpha}(\mathbf{k}_{\parallel})$ to a state with energy $\varepsilon_{\beta}(\mathbf{k}_{\parallel})$ with a probability $|\gamma_{\alpha\beta}|^2$. In this picture we consider only vertical transitions in \mathbf{k}_{\parallel} space. This means we are dealing with quasirect backscattering geometry and neglect any mechanism of

wave vector nonconservation. f_i in Eq. (4) means the Fermi-distribution function of the i th subband. Because of the \mathbf{k}_{\parallel} dependence of $\gamma_{\alpha\beta}$ [see also Fig. 2(b)] and $\varepsilon_i(\mathbf{k}_{\parallel})$ [see Fig. 2(a)] the shape and maximum position of single-particle intersubband excitations, which were described by Eq. (4), depend on the laser energy $\hbar\omega_i$.

Figure 3 displays calculated spectra of ($h_0 \rightarrow h_1$) single-particle intersubband excitations as schematically shown in Fig. 1(a) (heavy-hole transitions) for different laser energies $\hbar\omega_i$ for the same system as in Fig. 2. The vertical dashed lines mark the borders of the ($h_0 \rightarrow h_1$) single-particle continuum for vertical transitions [see also vertical arrows in Fig. 2(a)]. All calculated spectra, which are shown in Fig. 3, are normalized to unity for better comparison of the maximum positions. The calculations displayed in Fig. 3 clearly show that the ($h_0 \rightarrow h_1$) single-particle excitation energy, which can be observed by resonance Raman spectroscopy, depends on the energy $\hbar\omega_i$ of the incoming laser photons. Before resonance (negative $\Delta\hbar\omega_i$ in Fig. 3) the excitation energy of the ($h_0 \rightarrow h_1$) single-particle excitation is higher than in resonance ($\Delta\hbar\omega_i = 0$). After resonance ($\Delta\hbar\omega_i > 0$) the observable ($h_0 \rightarrow h_1$) energy again increases with increasing laser energy. $\Delta\hbar\omega_i$ means the detuning of the laser energy $\hbar\omega_i$ with respect to the subband spacing between the h_1 and the c_1 subbands at $\mathbf{k}_{\parallel} = \mathbf{0}$. The observation of the characteristic variation of the intersubband-transition energies with laser energy in experiment (see

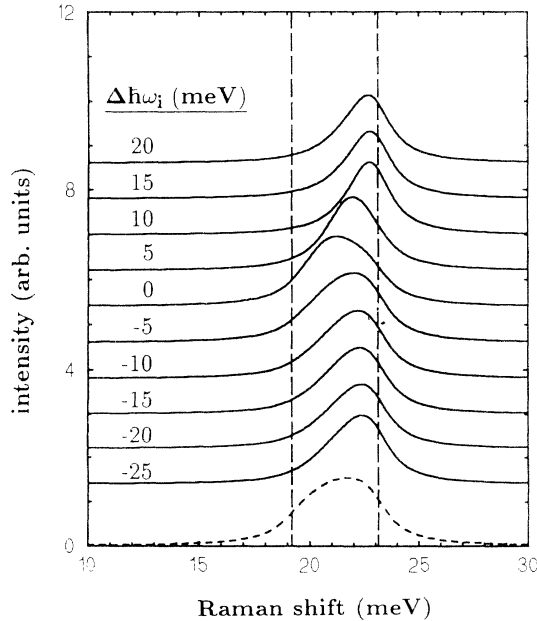


FIG. 3. Calculated and normalized ($h_0 \rightarrow h_1$) single-particle excitations of the same system as discussed in Fig. 2. The solid curves represent spectra, which are calculated with Eq. (4) and the results of Sec. II B for resonant excitation. $\Delta\hbar\omega_i$ gives the detuning of the laser energy $\hbar\omega_i$ relative to the energy of the subband spacing between the h_1 valence subband and the c_1 conduction subband. One recognizes the dependence of the line shape and maximum position of the ($h_0 \rightarrow h_1$) excitation from laser energy $\hbar\omega_i$. The dashed curve is calculated for nonresonant excitation for comparison.

below and Refs. 17 and 18) confirms the assumption that there is a strong single-particle scattering due to EDF's.

The 2D subband dispersion and wave functions used for the calculations presented in this publication were determined by solving Luttinger's 4×4 Hamiltonian.³⁴ The four coupled differential equations forming the Schrödinger equation were solved for the flat band case, which gives a good approximation for low doping concentrations.³⁵ For well thicknesses of the square-well potential around 100 Å and carrier concentrations $p \sim 10^{11} \text{ cm}^{-2}$ the effects of band bending on the calculated intersubband-transition energies are less than the experimental error ($< 0.1 \text{ meV}$). Thus for the sample parameters we used (see below), the effects of band bending can be neglected.

II. EXPERIMENTAL RESULTS

The experiments were performed in backscattering configuration at $T = 2 \text{ K}$ under resonant excitation using a tunable cw dye laser. The samples were immersed in liquid superfluid helium in a bath cryostat. The scattered light was analyzed with a triple spectrograph (DILOR XY) and a multichannel detector. The experimental results presented in this publication were derived from two samples. In Table I the essential parameters of the investigated p -type modulation-doped samples are listed. The samples were grown by molecular-beam epitaxy. Sample S is a one-side modulation-doped single quantum well. The undoped spacer of this structure is 200 Å thick and the doping area has a thickness of 60 Å. Sample M is a Be-doped multiple quantum-well structure containing 10 periods. The $\text{Ga}_{1-x}\text{Al}_x\text{As}$ barriers are 525 Å thick, with Be-doped center layers 35 Å thick. On sample M a $100 \mu\text{m} \times 100 \mu\text{m}$ mesa structure was etched for the experiments presented in Sec. II B.

A. Effects of subband nonparabolicity

Figure 4 shows a 3D plot of Raman spectra of the ($h_0 \rightarrow h_1$) intersubband excitation of sample S, the single quantum-well structure, in polarized scattering configuration for different laser energies. The dashed line marks the positions of the maxima of the ($h_0 \rightarrow h_1$) excitations. One can recognize the resonance behavior of the excitation. If the energy of the laser photons is in the vicinity of the band gap between the h_1 valence subband and the c_1 conduction subband, the observed Raman signal of the

TABLE I. Most important parameters of the samples investigated. The well widths L_z and 2D hole densities p were determined from our optical measurements (Sec. II A). This means p is the value of the carrier density under illumination. The Al contents x were taken from the growth parameters.

	Type	L_z (Å)	x	p (2 K) ($10^{11}/\text{cm}^2$)
Sample S	SQW	105	0.32	2.1 ± 0.2
Sample M	MQW	110	0.43	1.6 ± 0.2

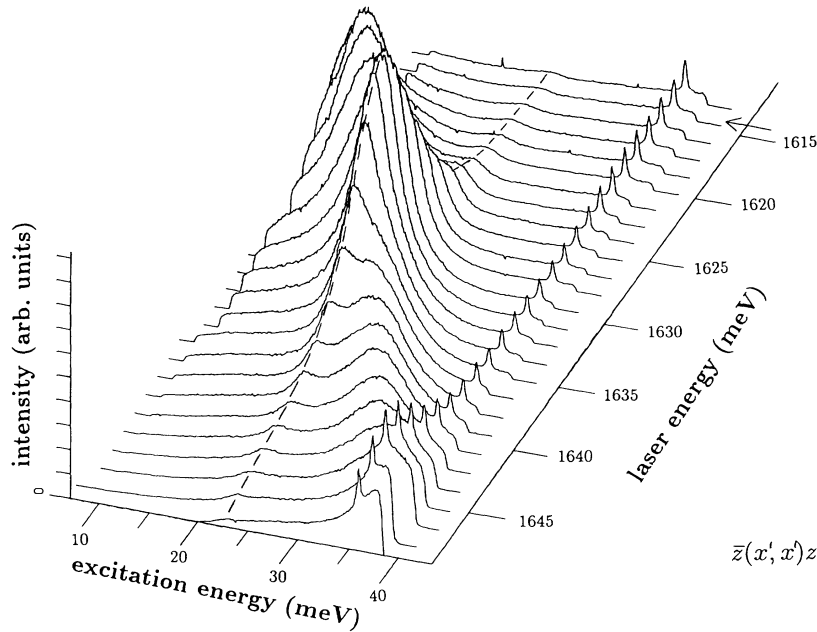


FIG. 4. Polarized Raman spectra of the ($h_0 \rightarrow h_1$) intersubband transition in sample S for different laser energies at $T \approx 1.8$ K. The dashed line marks the maximum positions of the ($h_0 \rightarrow h_1$) excitation. One can recognize the strong resonance behavior of this intersubband excitation. The sharp line at 36.6 meV is the GaAs LO phonon. The strong line, which crosses the plot, is the $c_1 \rightarrow h_0$ luminescence at constant absolute energy. An enlarged part of the spectrum which is marked with an arrow is displayed in Fig. 5.

($h_0 \rightarrow h_1$) transition shows a strong resonance enhancement. The sharp line at 36.6 meV is the LO phonon of GaAs. The strong line which crosses the picture comes from a luminescence transition from the c_1 conduction subband to the h_0 valence subband.

In Fig. 5 the depolarized and polarized spectra for a laser energy $E_L = 1614.8$ meV are shown. The polarized spectrum in Fig. 5 is an enlarged part of the spectrum, which is marked with an arrow in Fig. 4. The dashed line gives the calculated ($h_0 \rightarrow h_1$) SPE, which was calculated with Eq. (4) and the help of the results of Sec. II B. The observed excitations essentially have single-particle character due to Landau damping of the collective SDE's in depolarized geometry and the CDE's in the

polarized scattering configuration and resonant scattering by energy-density fluctuations (see above). In spite of the dominant single-particle character the excitations in depolarized and polarized spectra are slightly shifted against each other due to direct Coulomb interaction (depolarization shift). The vertical arrows in Fig. 5 give the maximum positions of the ($h_0 \rightarrow h_1$) excitations in depolarized and polarized scattering geometry. A remaining depolarization shift of roughly 1 meV can be deduced from the spectra in Fig. 5. Figure 6 shows the experimentally determined maximum positions of the ($h_0 \rightarrow h_1$) intersubband excitations in sample S versus laser energy for depolarized (open circles) and polarized (filled squares)

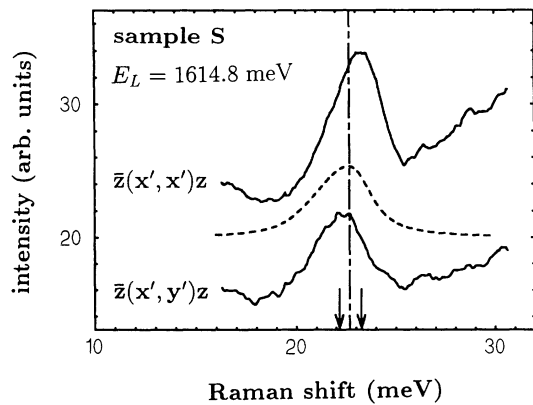


FIG. 5. Depolarized and polarized Raman spectra of the ($h_0 \rightarrow h_1$) intersubband excitation in sample S (solid lines). The vertical arrows mark the maximum positions respectively. The dashed line gives the calculated ($h_0 \rightarrow h_1$) SPE which was calculated with Eq. (4) and the help of the results of Sec. II B. Collective effects manifest themselves in the slight shift of the line centers (≈ 1 meV) relative to each other. The excitations mainly have single-particle character.

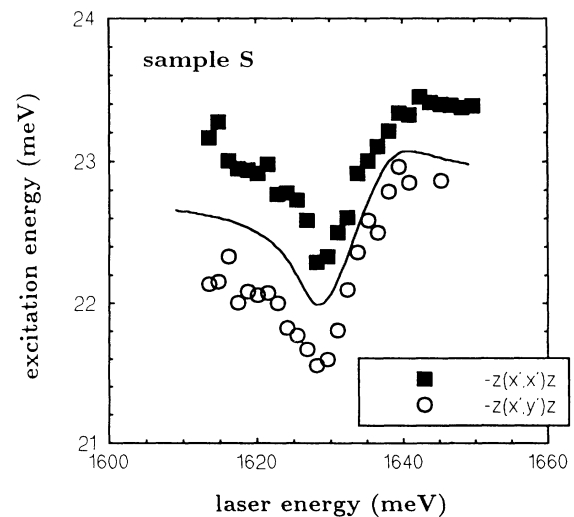


FIG. 6. Experimental values for the positions of the ($h_0 \rightarrow h_1$) SDE's (open circles) and the CDE's (filled squares) near resonance in sample S versus laser energy. Solid line: Maximum positions of the calculated SPE, using Eq. (4) and results of Sec. II B.

scattering configuration. The characteristic variation of the intersubband transition energies in depolarized as well as in polarized scattering configuration is caused by the nonparabolic subband dispersion^{17,18} [see Figs. 2(a) and 2(b)]. The solid line gives the theoretically calculated variation of the ($h_0 \rightarrow h_1$) SPE with laser energy which was calculated with Eq. (4) and the results of Sec. II B. It visualizes the variation of the maximum positions of the calculated single-particle spectra displayed in Fig. 3 with laser energy.

This characteristic variation of the observed ($h_0 \rightarrow h_1$) transition energies with laser energy can be understood in the following way. The Raman scattering probability is given by the product of the squares of the momentum matrix elements of the intersubband transitions participating in the scattering process, i.e., the ($h_1 \rightarrow c_1$) transition and the ($c_1 \rightarrow h_0$) transition [see Fig. 2(b)]. With the theoretical results displayed in Fig. 2 it follows that single-particle transitions around $\mathbf{k}_{\parallel} = \mathbf{0}$ do not significantly contribute to the observed Raman signal, whereas the contribution to the signal increases with increasing \mathbf{k}_{\parallel} . Off resonance, i.e., when the laser energy $\hbar\omega_i$ is well below the energy of the h_1 - c_1 band gap at $\mathbf{k}_{\parallel} = \mathbf{0}$, the most probable single-particle transitions around $\mathbf{k}_{\parallel} = \mathbf{k}_F$, with energies higher than those around $\mathbf{k}_{\parallel} = \mathbf{0}$, dominate the observed spectrum. If the laser energy reaches the value of the h_1 - c_1 band gap, transitions around $\mathbf{k}_{\parallel} = \mathbf{0}$ are resonantly enhanced and the observed ($h_0 \rightarrow h_1$) transition energy decreases accordingly. If the laser energy is above the h_1 - c_1 band gap at $\mathbf{k}_{\parallel} = \mathbf{0}$, the maximum position of the observed ($h_0 \rightarrow h_1$) transition increases with increasing laser energy, because the h_0 - h_1 subband spacing also increases with increasing \mathbf{k}_{\parallel} [see Fig. 2(a)]. Above resonance, i.e., when the laser energy is above the energy of the h_1 - c_1 band gap at $\mathbf{k}_{\parallel} = \mathbf{k}_F$, the spectrum is again dominated by the most probable transitions around $\mathbf{k}_{\parallel} = \mathbf{k}_F$. The increasing branch of the theoretical curve in Fig. 6 is mainly determined by the Fermi wave vector \mathbf{k}_F . So from the fit of the theoretical curve to the experimental data the carrier concentration $p = k_F^2/2\pi$ under illumination can be determined with quite good accuracy (see Table I).

We have observed similar variations of the ($h_0 \rightarrow h_1$) transition energies with laser energy in various other samples with well widths around 100 Å (not published here). In a sample with $L_z \sim 200$ Å the ($h_0 \rightarrow h_2$) intersubband excitation could be observed.¹⁸ These investigations are interesting, because the curvature of the h_2 subband has a sign opposite to that of the h_1 subband. Correspondingly the variation of the intersubband-transition energy with laser energy is different for the ($h_0 \rightarrow h_1$) and the ($h_0 \rightarrow h_2$) excitation.¹⁸ The fact that the variation of the observed excitation energies with laser energy can be explained quite well by the behavior of calculated single-particle spectra demonstrates that the observed excitations have essentially single-particle character. As stated above in Sec. I this strong single-particle scattering can be understood in terms of scattering by energy-density fluctuations under conditions of extreme resonance. Furthermore, the observed excitations lie within the continuum of single-particle excitations and hence the collec-

tive parts suffer Landau damping (see Fig. 7). The vertical shift between the excitation energies in depolarized and polarized configuration in Fig. 6 is the depolarization shift. This shift is a consequence of the remaining collective part of the observed excitations, e.g., SDE's and CDE's. The collective effects are further investigated in Sec. II B.

Figure 7 shows the variation of the ($h_0 \rightarrow h_1$) intersubband-transition energies of sample M versus laser energy. The solid line gives the calculated variation of the ($h_0 \rightarrow h_1$) SPE which was for the time being fitted to the experimental points in depolarized scattering configuration. The dashed lines mark the borders of the single-particle continuum for vertical transitions. This shows, as already mentioned, that the observed excitations lie within the single-particle continuum and hence suffer Landau damping.

B. Effects of many-particle interactions

To test the relative strengths of direct and exchange Coulomb interaction in the 2D hole gas, we have performed experiments under variation of the carrier density p by illuminating a $100 \mu\text{m} \times 100 \mu\text{m}$ mesa (sample M) with an additional Ar laser ($\lambda = 514 \text{ nm}$). The energy of the green Ar-laser line was well above the band gap of the $\text{Ga}_{1-x}\text{Al}_x\text{As}$ barriers, so that electron-hole pairs have been generated in the barriers. The reduction of the density of the 2D hole gas in the wells is very similar to a mechanism which was reported by Jusserand *et al.* for n -type modulation-doped quantum wells.³⁶ In our experiments the mesa structure was nearly homogeneously illuminated by an Ar-laser spot of about $200 \mu\text{m}$ diameter. The Raman signals were recorded from a dye-laser spot of about $50 \mu\text{m}$ diameter in the center

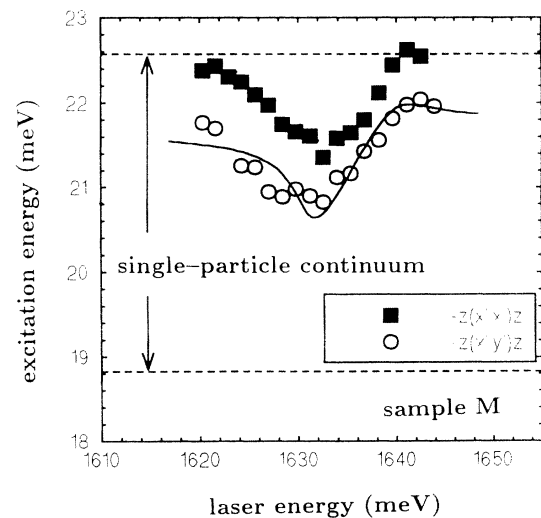


FIG. 7. Same as Fig. 6, but for sample M. The solid line was fitted to the experimental values in depolarized geometry. The dashed lines give the upper and lower limits of the ($h_0 \rightarrow h_1$) single-particle continuum for vertical transitions [see also arrows in Fig. 2(a)].

of the mesa. The power density of the dye-laser beam was about 200 W cm^{-2} , whereas the power density in the Ar-laser beam was varied between 0 and 2 W cm^{-2} . While the additional photogenerated holes remain in the valence band of the barriers, their electron partners are transferred into the wells, where they recombine radiatively with some carriers of the 2D hole gas. By the additional illumination the 2D hole density p in the quantum wells could be reduced to a value of about 60% of the carrier density in the dark. The actual value of p was estimated from the band-gap renormalization^{37,38} (BGR). The BGR was experimentally determined as the difference of the calculated single-particle subband spacing between the h_0 valence band and the c_0 conduction band and the corresponding luminescence energy. More recent investigations^{39,40} indicate, however, that excitonic effects are not negligible at hole densities of about $2 \times 10^{11} \text{ cm}^{-2}$. In *p*-doped samples they seem to play a more dominant role than in *n*-doped samples, where at densities of about 10^{11} cm^{-2} excitonic interactions are almost screened. Therefore the amount of the reduction of the 2D hole density by additional illumination given here, which was determined by the interpretation of a corresponding shift of the quantum-well luminescence as an effect of the BGR only without considering excitonic effects, must be seen as a lower limit. One may find a stronger decrease of the 2D hole density by additional illumination (up to a factor of about 2) if excitonic effects are considered in the calculations.

Figure 8 shows the variation of the ($h_0 \rightarrow h_1$) intersubband-transition energies in depolarized and polarized scattering configuration with p . These energies were determined as the average of all transition energies measured for a large number of laser energies in the range of the resonance of the Raman process, as for example displayed in Fig. 7. The dashed line represents the variation of the average ($h_0 \rightarrow h_1$) single-particle energy calculated with the help of Eq. (4) and a $\mathbf{k} \cdot \mathbf{p}$ subband calculation as described above. The decrease of the aver-

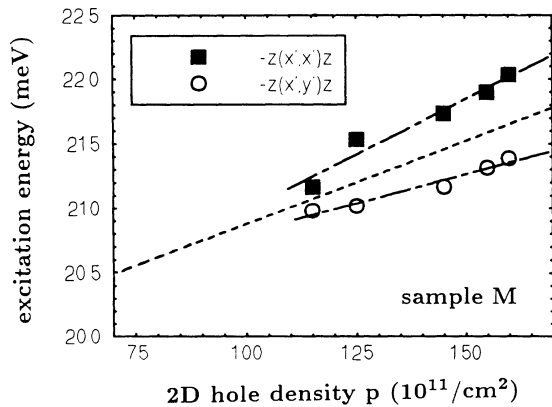


FIG. 8. Averaged energies of the ($h_0 \rightarrow h_1$) SDE's (open circles) and CDE's (filled squares) for different 2D hole densities p in sample M around the $h_1 \rightarrow c_1$ resonance. The dashed line describes the calculated decrease of the ($h_0 \rightarrow h_1$) single-particle energy with decreasing p . The dashed-dotted lines are guides to the eye.

age single-particle energy with decreasing hole density p is caused by the nonparabolicity of the 2D valence subbands and the decrease of the Fermi wave vector \mathbf{k}_F [see Fig. 2(a)]. The dashed-dotted lines are guides to the eye. The well width of the investigated structure was determined in the following way. For the spectra series with minimal 2D hole density there is only an almost vanishing depolarization shift between the excitation energies in depolarized and polarized spectra observable (marks at $p = 1.15 \times 10^{11} \text{ cm}^{-2}$ in Fig. 8). The spectra are nearly complete single-particle spectra. The well width was determined to $L_z = 105 \text{ \AA}$ by fitting a theoretical curve, as for example displayed in Figs. 6 and 7, to the experimental values (not displayed here). Figure 8 shows that for $p < 10^{11} \text{ cm}^{-2}$ the spectra should be complete single-particle spectra with vanishing depolarization shift. Figure 8 also shows that the excitations in polarized and in depolarized configuration are shifted symmetrically with respect to the calculated SPE (dashed line). For an estimation of the relative strength of direct and exchange Coulomb interaction we use relations which were derived theoretically for the energies of collective SDE's and CDE's of the 2D electron gas of *n*-type modulation-doped GaAs/Ga_xAl_{1-x}As quantum-well structures:⁶

$$\hbar\Omega_{\text{SDE}} = \hbar\Omega_{01} - \beta_{01}, \quad (5)$$

$$\hbar\Omega_{\text{CDE}} = \hbar\Omega_{01} + \alpha_{01} - \beta_{01}, \quad (6)$$

where $\hbar\Omega_{01}$ means the (constant) energy of a SPE and α_{01} (β_{01}) is the parameter of the direct (exchange) Coulomb interaction.¹¹ Using Eqs. (5) and (6) the results displayed in Fig. 8 yield a ratio of 2:1 for $\alpha_{01}:\beta_{01}$. If we take the excitonic effects in the luminescence transitions into account, a ratio of almost 1:1 for $\alpha_{01}:\beta_{01}$ may follow, because the reduction of the 2D hole density may have been underestimated. Therefore a ratio, which lies between 2:1 and 1:1, can be deduced from our experiments. The uncertainty comes from the error in the determination of the 2D hole density. Nevertheless our experiments yield a stronger relative strength of the exchange interaction in comparison to the direct Coulomb interaction than was found for 2D electron gases in *n*-type modulation-doped GaAs/Ga_{1-x}Al_xAs quantum-well structures by Pinczuk *et al.*¹¹ (2.5:1 for $\alpha_{01}:\beta_{01}$). This might be more understandable if we take into consideration that the holes have a larger effective mass than the electrons: From electrons in Si-inversion layers a considerable influence of the exchange interaction on the band structure is known.² The effective mass of electrons in Si-inversion layers is large compared to the effective mass of electrons in GaAs.

III. CONCLUSION

In conclusion we have investigated intersubband excitations of the 2D hole gas in *p*-doped GaAs/Ga_xAl_{1-x}As quantum-well structures by means of resonance Raman spectroscopy. The observed excitations have essentially single-particle character due to Landau damping of collective SDE's and CDE's and the resonant scattering by

energy-density fluctuations. An estimate of the relative strengths of direct and exchange Coulomb interaction in the 2D hole gas in GaAs/Ga_{1-x}Al_xAs quantum-well structures with $L_z \sim 100 \text{ \AA}$ and $p \sim 10^{11} \text{ cm}^{-2}$ has been given. It was found that exchange Coulomb interaction is presumably more dominant than in 2D electron gases.

ACKNOWLEDGMENTS

The authors are grateful for valuable discussions with E. Bangert and V. Latussek and to M. Emmerling, who has prepared the mesa structures. The Deutsche Forschungsgemeinschaft has supported this work.

- ¹ D. A. Dahl and L. J. Sham, *Phys. Rev. B* **16**, 651 (1977).
- ² T. Ando, A. B. Fowler, and F. Stern, *Rev. Mod. Phys.* **54**, 437 (1982).
- ³ T. Ando and S. Katayama, *J. Phys. Soc. Jpn.* **54**, 1615 (1985).
- ⁴ G. Eliasson, P. Hawrylak, and J. J. Quinn, *Phys. Rev. B* **35**, 5569 (1987).
- ⁵ A. C. Tselis and J. J. Quinn, *Phys. Rev. B* **29**, 3318 (1984).
- ⁶ M. Y. Jiang, *Solid State Commun.* **84**, 81 (1992).
- ⁷ M. S.-C. Luo, S. L. Chuang, S. Schmitt-Rink, and A. Pinczuk, *Phys. Rev. B* **48**, 11086 (1993).
- ⁸ L. D. Landau, *J. Phys. (USSR)* **10**, 25 (1946).
- ⁹ C. Schüller, J. Kraus, V. Latussek, and J. K. Ebeling, *Solid State Commun.* **81**, 3 (1992).
- ¹⁰ L. Wondler, *Solid State Commun.* **65**, 1197 (1988).
- ¹¹ A. Pinczuk, S. Schmitt-Rink, G. Danan, J. P. Valadares, L. N. Pfeiffer, and K. W. West, *Phys. Rev. Lett.* **63**, 1633 (1989).
- ¹² D. Gammon, B. V. Shanabrook, J. C. Ryan, and D. S. Katzer, *Phys. Rev. B* **41**, 12311 (1990).
- ¹³ D. Gammon, B. V. Shanabrook, J. C. Ryan, G. Brozak, and D. S. Katzer, *Surf. Sci.* **263**, 471 (1991).
- ¹⁴ D. Gammon, B. V. Shanabrook, J. C. Ryan, D. S. Katzer, and M. J. Yang, *Phys. Rev. Lett.* **68**, 1884 (1992).
- ¹⁵ Hong Yu and J. C. Hermanson, *Phys. Rev. B* **43**, 4340 (1991).
- ¹⁶ M. Altarelli, U. Ekenberg, and A. Fasolino, *Phys. Rev. B* **32**, 5138 (1985).
- ¹⁷ M. Kirchner, C. Schüller, J. Kraus, G. Schaack, and G. Weimann, in *Proceedings of the 13th International Conference on Raman Spectroscopy*, edited by W. Kiefer *et al.* (Wiley, Chichester, 1992), p. 842.
- ¹⁸ M. Kirchner, C. Schüller, J. Kraus, G. Schaack, K. Panzlauff, and G. Weimann, *Phys. Rev. B* **47**, 9706 (1993).
- ¹⁹ A. Pinczuk, H. L. Störmer, A. C. Gossard, and W. Wiegmann, in *Proceedings of the 17th International Conference on the Physics of Semiconductors*, edited by J. D. Chadi and W. Harrison (Springer, Berlin, 1985), p. 329.
- ²⁰ T. Ando, *J. Phys. Soc. Jpn.* **54**, 1528 (1985).
- ²¹ G. Brozak, B. V. Shanabrook, D. Gammon, and D. S. Katzer, *Phys. Rev. B* **47**, 9981 (1993).
- ²² R. K. Hayden, G. K. Maude, L. Eaves, E. C. Valadares, M. Henini, F. W. Sheard, O. G. Hughes, J. C. Portal, and L. Cury, *Phys. Rev. Lett.* **66**, 1749 (1991).
- ²³ M. Zachau, J. A. Kash, and W. T. Masselink, *Phys. Rev. B* **44**, 4048 (1991).
- ²⁴ M. Zachau, M. A. Tischler, and U. Ekenberg, *Phys. Rev. Lett.* **69**, 2260 (1992).
- ²⁵ R. K. Hayden, L. Eaves, M. Henini, T. Takamasu, N. Miura, and U. Ekenberg, *Appl. Phys. Lett.* **61**, 84 (1992).
- ²⁶ R. K. Hayden, E. C. Valadares, L. Eaves, M. Henini, D. K. Maude, and J. C. Portal, *Phys. Rev. B* **46**, 15586 (1992).
- ²⁷ A. Pinczuk, D. Heiman, R. Sooryakumar, A. C. Gossard, and W. Wiegmann, *Surf. Sci.* **170**, 573 (1985).
- ²⁸ E. Burstein, A. Pinczuk, and D. L. Mills, *Surf. Sci.* **98**, 451 (1980).
- ²⁹ D. Hamilton and A. L. McWhorter, in *Light Scattering Spectra of Solids*, edited by G. B. Wright (Springer, New York, 1969), p. 309.
- ³⁰ P. A. Wolff, in *Light Scattering Spectra of Solids* (Rev. 29), p. 309.
- ³¹ M. V. Klein, in *Light Scattering in Solids*, edited by M. Cardona (Springer, Berlin, 1975), p. 147.
- ³² F. A. Blum, *Phys. Rev. B* **1**, 1125 (1970).
- ³³ G. Abstreiter, M. Cardona, and A. Pinczuk, in *Light Scattering in Solids IV*, edited by M. Cardona and G. Güntherodt (Springer, Berlin, 1984), p. 5.
- ³⁴ J. M. Luttinger and W. Kohn, *Phys. Rev.* **97**, 869 (1955).
- ³⁵ U. Ekenberg and M. Altarelli, *Phys. Rev. B* **32**, 3712 (1985).
- ³⁶ B. Jusserand, J. A. Brum, D. Gardin, H. W. Liu, G. Weimann, and W. Schlapp, *Phys. Rev. B* **40**, 4220 (1989).
- ³⁷ D. A. Kleinman and R. C. Miller, *Phys. Rev. B* **32**, 2266 (1985).
- ³⁸ C. Delalande, G. Bastard, J. Orgonasi, J. A. Brum, H. W. Liu, and M. Voos, *Phys. Rev. Lett.* **59**, 2690 (1987).
- ³⁹ H. Akiyama, T. Matsusue, and H. Sakahi, *Phys. Rev. B* **49**, 14523 (1994).
- ⁴⁰ R. Hartmann and J. Kraus (unpublished).